

# Sheet necking prediction in forming limit diagrams with the anisotropy influence incorporation

**P Farahnak, A Prantl, J Dzugan, P Konopik and R Prochazka**

COMTES FHT a.s., Průmyslová 995, 334 41 Dobřany, Czech Republic

E-mail: pedram.farahnak@comtesfht.cz

**Abstract.** A well-known method of materials formability description is the Forming Limit Diagram (FLD). In FLDs/FLC (Forming Limit Curve) a plot of major and minor principal strains in the plane of deformed sheet where necking takes place is represented. The current paper is dealing with anisotropy influence on FLC. This effect is going to be studied with the use of mild steel DC01. Hills anisotropic criterion is considered here and for its application experimental investigation has to be carried out in order to provide input data for the model applied. Uniaxial tensile tests were performed for basic characterisation of sheet samples with the use of contact-less measuring devices. In order to assess the anisotropy experimentally, the specimens were extracted and tested in Rolling Direction (RD), Transverse Direction (TD) and 45° Skew Direction (SD) for the Lankford ratios determination. Detailed stress state description of the material investigated was carried out with the use the stress triaxiality and Lode angle parameter. Therefore, transformations from conventional space into stress state provide a profound insight into the necking phenomenon. According to the experimental and numerical results it was found that it is necessary to take anisotropy effects into account for the material investigated.

## 1 Introduction

A well-known method of materials formability description is the FLD. The concept was firstly introduced by Keeler [1] and stands as the first safety criterion in deep drawing operations and it is still a conventional approach to assess sheets formability. Based on a deeper analysis of explanatory power of FLD diagram, one can see that it shows the representation of the deformability from a practical-technical point of view rather than from the perspective of ductile damage. In FLDs/FLC a plot of major and minor principal strains in the plane of deformed sheet where necking takes place is represented. Although this concept is very simple and well understood for proportional loading, its experimental determination is rather complex demanding a wide range of sheet metal forming tests. A large number of theories for predicting of sheet necking have been proposed, which can be differentiated in two main theoretical frameworks: the necking theory in homogeneous sheets, based on the original work developed in [2, 3] and the theory of sheet non-homogeneity proposed by Marciniak and Kuczynski (M-K) [4].

From technical and practical points of view, fracture experiments are evaluated in the space of equivalent plastic strain, stress triaxiality and Lode angle parameter that can be obtained by conversion from conventional space. It can be defined and calibrated under the proportional



loading using an assumption that the ratio of two principal strain increments is constant. In equation (1),

$$\alpha = \frac{d\varepsilon_2}{d\varepsilon_1} \quad (1)$$

Subsequently, the transformation into another spaces based on plane stress plasticity formulas is considered.

## 2 Theoretical fundamentals

### 2.1 Transformation of conventional FLD into the stress state space under plane stress

For proportional loading path, the increments of principal plastic strains follow the equation:

$$d\varepsilon_1 : d\varepsilon_2 : d\varepsilon_3 = 1 : \alpha : -(1 + \alpha) \quad (2)$$

Where the material is considered to be incompressible and isotropic. The material is assumed to obey equivalent stress and the associated flow rule,

$$\begin{aligned} \bar{\sigma} &= \sqrt{\frac{1}{2}[(\sigma_1 - \sigma_2)^2 + (\sigma_2 - \sigma_3)^2 + (\sigma_3 - \sigma_1)^2]} \\ d\varepsilon_{ij} &= d\Lambda \frac{\partial \bar{\sigma}}{\partial \sigma_{ij}} = \frac{3}{2} \frac{d\Lambda}{\bar{\sigma}} s_{ij} \end{aligned} \quad (3)$$

Where  $\sigma_{ij}$  are stress components,  $\sigma_1, \sigma_2$  and  $\sigma_3$  are principal stresses,  $s_{ij}$  are deviatoric stress components,  $d\Lambda$  is the plastic multiplier, and  $d\varepsilon_{ij}$  is the plastic strain increments. For simplicity, the equation (3) is assumed to hold for both positive and negative  $\alpha$  values. The stress ratios can be defined as,

$$\frac{\sigma_2}{\sigma_1} = \beta ; \frac{\sigma_3}{\sigma_1} = \gamma \quad (4)$$

The second term of equation (3) can also be written in the principal stress and strain space, and after some substitutions, the stress triaxiality  $\lambda$ , the Lode angle parameter  $\bar{\theta}$  and necking strain  $\bar{\varepsilon}$  can be expressed in terms of the stress ratio  $\beta$  and  $\alpha$ :

$$\begin{aligned} \lambda = \frac{\sigma_m}{\bar{\sigma}} &= \frac{\beta + 1}{3\sqrt{\beta^2 - \beta + 1}} ; \bar{\theta} = 1 - \frac{2}{\pi} \arccos \xi = 1 - \frac{2}{\pi} \arccos \left[ \frac{(\beta + 1)(\beta - 2)(2\beta - 1)}{2(\beta^2 - \beta + 1)^{3/2}} \right] \\ \bar{\varepsilon} &= \frac{2\varepsilon_1}{\sqrt{3}} \sqrt{1 + \alpha + \alpha^2} \end{aligned} \quad (5)$$

Where  $\xi$  defined by equation (6) is the normalized third deviatoric stress invariant of the stress tensor and  $\sigma_m$  is the mean stress (for more details see [5-11]).

$$\xi = \frac{27}{2} \frac{(\sigma_1 - \sigma_m)(\sigma_2 - \sigma_m)(\sigma_3 - \sigma_m)}{\bar{\sigma}^3} \quad (6)$$

## 2.2 Plasticity model parameter identification

Plasticity behaviour of isotropic material or von Mises yield criterion has been studied vastly in numerous researches. In this case, elastic properties (Young's modulus and Poisson's ratio) as well as plastic properties such as yield stress and hardening behaviour have been assumed independent of material orientation. However, in many circumstances of practical interest, material behaviour is truly anisotropic with substantial discrepancy among phenomenological properties observed in different material directions. From technical and practical points of view, the isotropy assumption may lead to a poor representation of the actual behaviour. Therefore the formulation and use of appropriate anisotropic plasticity model could raise the accuracy in finite element predictions. A well-known orthotropic model proposed by Hill (1948) is introduced here [12].

### 2.2.1 Hill orthotropic model

The Hill criterion can be considered as an orthotropic extension of von Mises criterion which provides model with the material anisotropic behaviour. Stress tensor components are denoted by  $\sigma_{ij}$ . The rolling, transverse and thickness directions of the sheet are defined on an orthonormal basis and designated as  $x$ ,  $y$  and  $z$ . The yield function associated with the Hill criterion can be expressed by following equation (7):

$$\begin{aligned} \varphi(\sigma, \bar{\sigma}) = & F(\sigma_{xx} - \sigma_{yy})^2 + G(\sigma_{zz} - \sigma_{xx})^2 + H(\sigma_{xx} - \sigma_{yy})^2 \\ & + 2L\sigma_{yz}^2 + 2M\sigma_{zx}^2 + 2N\sigma_{xy}^2 - \bar{\sigma}^2 \end{aligned} \quad (7)$$

Here,  $F$ ,  $G$ ,  $H$ ,  $L$ ,  $M$  and  $N$  are anisotropic coefficients, which were calibrated using three R-values ( $r_0, r_{45}, r_{90}$ ) or Lankford ratios.

$$F = \frac{r_0}{r_{90}(1+r_0)}; \quad G = \frac{1}{1+r_0}; \quad H = \frac{r_0}{1+r_0}; \quad N = \frac{(r_0+r_{90})(2r_{45}+1)}{2r_{90}(1+r_0)} \quad (8)$$

In section 3, measurement of Hill's coefficients from uniaxial tensile test will be discussed.

## 3 Experiment description

The material investigated is a mild steel DC01 and tensile experiments were performed on different specimen geometries. Figure 1(a) depicts uniaxial tensile test specimen with thickness 1.5 mm that is used for necking prediction. However, in order to characterize the Lankford ratios and subsequently Hill's coefficients in equation (8), it is necessary to perform uniaxial tests on the sample of the same thickness which are extracted in RD, TD and SD. Figure 1 (b) indicates the extractions of samples along aforementioned sampling directions. All the experiments were conducted by constant velocity 4 mm/min and through the experiments, displacement fields are monitored using Digital Image Correlation (DIC) system. In particular, the evolution of width strain is determined by using virtual extensometer. After computing the logarithmic plastic strains in the width and thickness directions (assuming plastic incompressibility), the Lankford ratios were determined from the average slopes,

$$r = \frac{d\varepsilon_w^p}{d\varepsilon_{th}^p} \quad (9)$$

Tables 1 and 2 summarize the identified anisotropy's constants and material properties including Swift Hardening Law (SHL), respectively.

**Table 1.** Lankford ratios and Hill's coefficients.

$r_0$	$r_{45}$	$r_{90}$	$F$	$G$	$H$	$L$	$M$	$N$
1.66	1.24	2.02	0.30	0.37	0.62	1.5	1.5	1.19

**Table 2.** Material Properties.

$E$	$\nu$	$\sigma_y$	SHL	$A$	$\varepsilon_0$	$n$
200(GPa)	0.3	180(MPa)	$K = A(\bar{\varepsilon}_p + \varepsilon_0)^n$	625(MPa)	0.62	1.19

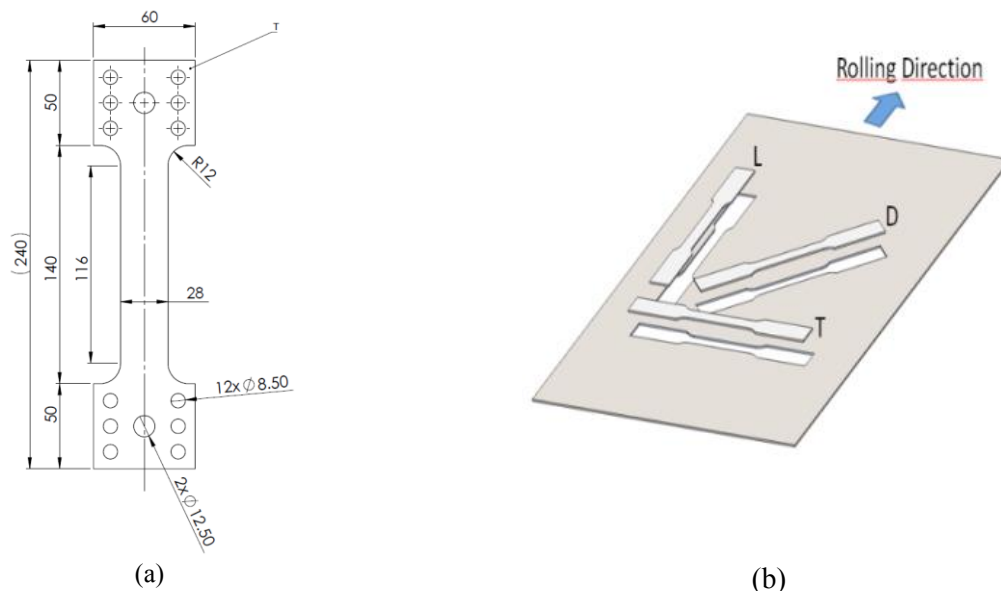


**Figure 1.** (a) Uniaxial tensile test specimen; (b). Sampling directions for Lankford ratios identification.

#### 4 Numerical simulation

The aim of numerical simulation is to predict the necking by using isotropic and anisotropic material modelling. For this sake, numerical reaction force-displacement curves are obtained and compared with the experimental data. Figure 2(a) represents the behaviour of the material along the boundary condition. It is noticeable that during the experiment, reaction force and displacement were measured by testing machine in both heads of the specimen and the same boundary condition is imposed for the numerical simulations. In addition, it is shown in figure 2(b) in the necking zone the major and minor strains were measured with the use of the DIC. The same variable is evaluated in the numerical simulations for comparison. Moreover, figure 2(c) indicates the obtained result from the Nakajima test for DC01. Finally, figure 2(d) is the transformation of the Nakajima based on the formulations in section 2.1, however, the range of interest for this paper is only between points **c** and **d** in which stress

triaxiality and Lode angle parameter vary from  $0.33 < \lambda < 0.57$  and  $0 < \bar{\theta} < 1$ , respectively [13-17]. The obtained numerical results from anisotropic material modelling reflect the actual behaviour of the material, while the results of isotropic simulation significantly deviate from the experimental results. Therefore, for material DC01 anisotropy effects must be considered even for uniaxial tensile test.

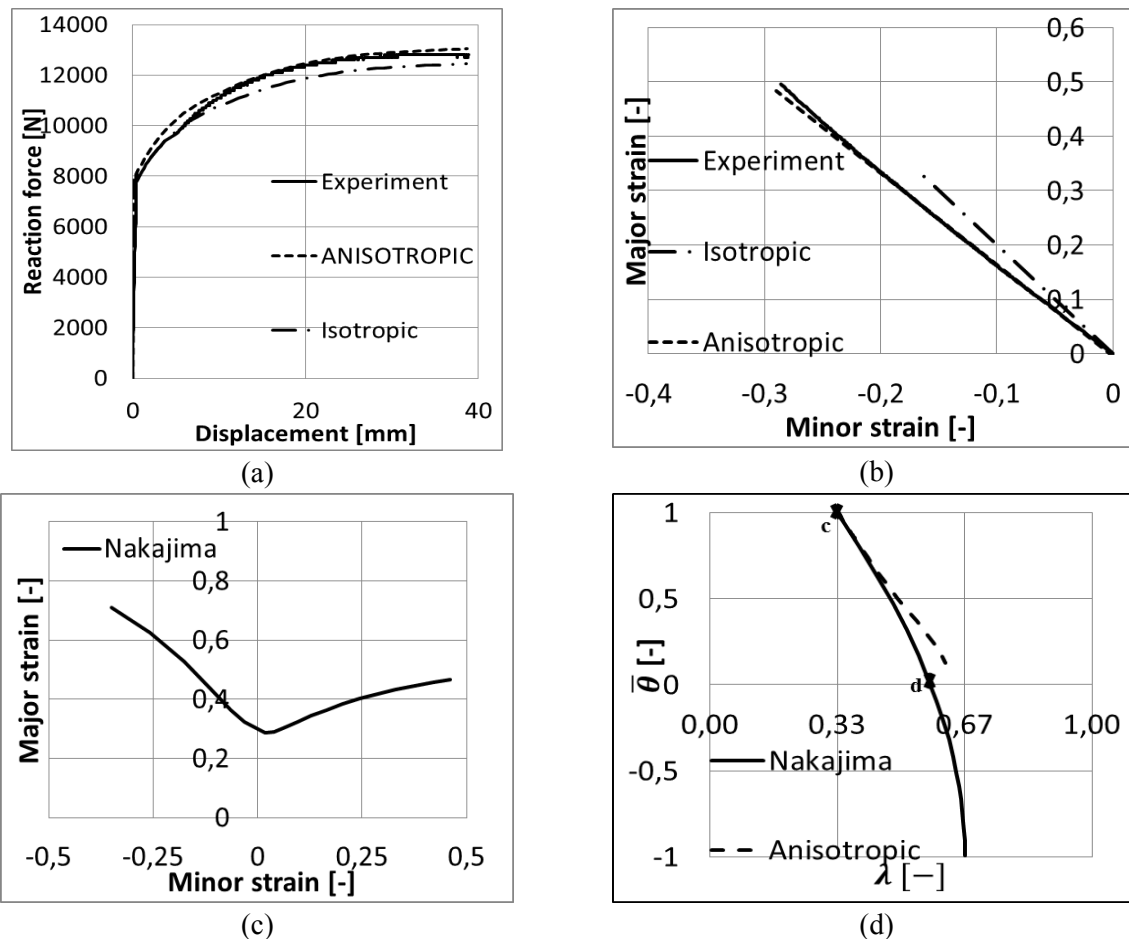


**Figure 2.** (a) and (b) evaluation along the boundary condition and necking zone, respectively; (c) FLC from Nakajima test; (d) transformation of the FLD into the stress state space.

## 5 Conclusion

In order to characterize Hill's anisotropy coefficients, it was a prerequisite to extract samples from the sheet of mild steel DC01 with the same thickness 1.5 mm. The obtained results for reaction force-displacement as well as conventional FLD for a critical node inside the necking zone demonstrate that anisotropic FEM simulation represents the actual behavior of the material. Moreover, for obtaining the whole forming curve of mild steel DC01, many Nakajima test with a variety of widths were performed which can only be represented in the conventional space. Therefore, it is possible to transform it into stress state spaces which comprise necking strain, stress triaxiality and Lode angle parameter. Furthermore, in order to cover the whole FLC, plane strain tension and equi-biaxial tension have to be performed with another alternative, like a cruciform specimen in the future research.

## Acknowledgements

This paper was created by project TF02000072 - Methods development for formability assessment of thin sheets considering anisotropy and non-linear loading path (2016-2019, TA0/TF) financed by the Technology Agency of the Czech Rep. and project Development of West-Bohemian Centre of Mat.and Metal. No.: LO1412, financed by the MEYS of the Czech Rep.

## References

- [1] Keeler S P and Backofen W 1963, Plastic instability and fracture in sheets stretched over rigid punches *Transactions of American Society for Metals*, vol. **56**, pp. 25-48,.
- [2] Hill R 1952 On discontinuous plastic states, with special reference to localized necking in thin sheets *mechanics and Physics of Solids*, vol. **1**, no. 1, pp. 19-30.
- [3] Swift W 1952 Plastic instability under plane stress *Mechanics and Physics of Solids*, vol. **1**, no. 1, pp. 1-18.
- [4] Marciniak Z and Kuczyski K 1967 Limit strains in the processes of stretch-forming sheet metal *Mechanical Sciences*, vol. **9**, no. 9, pp. 609-620,.
- [5] Stoughton TB 2000 A general forming limit criterion for sheet metal forming *International Journal of Mechanical Sciences*, vol. **42**, no. 1, pp. 1-27.
- [6] Lee YW 2005 Fracture predictions in metal sheets PhD thesis, Massachusetts Institute of technology,.
- [7] Bai Y and Wierzbicki T 2008 Forming severity concept for predicting sheet necking under complex loading histories *International Journal of Mechanical Science*, vol. **50**, pp.1012-22
- [8] Bai Y and Wierzbicki T 2008 A new model of metal plasticity and fracture with pressure and Lode dependence *International Journal of Plasticity*, vol. **24**, no. 6, pp. 1071-96,.
- [9] Bai Y and Wierzbicki T Application of Mohr-Coulomb criterion to ductile fracture *Report*
- [10] Hooputra H Gese H Dell H Werner H and Health A 2003 A new comprehensive failure model for crashworthiness simulation-validation for aluminum extrusions *In: 13<sup>th</sup> European Conference on Digital Simulation for Virtual Prototyping, Virtual Manufacturing and Virtual Environment*, Mainz, Germany, October.
- [11] Hooputra H Gese H Dell H and Werner H 2007 A comprehensive failure model for crashworthiness of aluminum extrusions *International Journal of Crashworthiness*, vol. **9**, pp. 449-64.
- [12] Souza E A Perić D Owen D R J 2008 Computational Methods for Plasticity: Theory and Applications Swansea University, *John Wiley and Sons Publications*, ISBN: 9780470694527, pp. 414-16,.
- [13] Hari C Gholipour J Bardelick A and Worswick MJ 2007 Prediction of necking in tabular hydroforming using an extended stress-based forming limit curve *Journal of Engineering Materials and Technology*, vol. **129**, pp. 36-47,.
- [14] Mohr D and Marcadet J 2015 Micromechanically-motivated phenomenological Hosford-Coulom model for predicting ductile fracture initiation at low stress triaxialities *International Journal of Solids and Structures*, vol. **67**, pp. 40-55.
- [15] Kubík P, Šebek F, Petruška J, Hůlka J, Růžicka J, Španiel M, Džugan J, Prantl A 2013 Calibration of Selected Ductile Fracture Criteria Using Two Types of Specimens, *Key Engineering Materials*, ISSN: 1662-9795, Vol. **592-593**, pp.258-261.
- [16] Španiel M, Prantl A, Džugan J, Růžicka J, Moravec M, Kuželka J 2014 Calibration of fracture locus in scope of uncoupled elastic-plastic-ductile fracture material models, *Advances in Engineering Software*, Vol. **72**, pp.95-108
- [17] Džugan J, et al 2015 Identification of ductile damage parameters for pressure vessel steel. *Nucl. Eng. Des.*, <http://dx.doi.org/10.1016/j.nucengdes.2015.12.014>